## General Disclaimer

## One or more of the Following Statements may affect this Document

- This document has been reproduced from the best copy furnished by the organizational source. It is being released in the interest of making available as much information as possible.

- This document may contain data, which exceeds the sheet parameters. It was furnished in this condition by the organizational source and is the best copy available.

- This document may contain tone-on-tone or color graphs, charts and/or pictures, which have been reproduced in black and white.

- This document is paginated as submitted by the original source.

- Portions of this document are not fully legible due to the historical nature of some of the material. However, it is the best reproduction available from the original submission.

**NASA TECHNICAL MEMORANDUM**

NASA TM X-62,456

NASA TM X-62,456

# DIRECT OBSERVATION OF SMALL CLUSTER MOBILITY AND RIPENING

**Klaus Heinemann**
**and**
**Helmut Poppa**

**Ames Research Center**
**Moffett Field, Calif. 94035**



**July 1975**

| 1. Report No. | 2. Government Accession No. | 3. Recipient's Catalog No. |
|---|---|---|
| NASA TM X-62,456 | | |

| 4. Title and Subtitle | 5. Report Date |
|---|---|
| Direct Observation of Small Cluster Mobility and Ripening | 6. Performing Organization Code |
| 7. Author(s) | 8. Performing Organization Report No. |
| Klaus Heinemann and Helmut Poppa | A-6173 |
| 9. Performing Organization Name and Address | 10. Work Unit No. |
| NASA-Ames Research Center<br>Moffett Field, California 94035 | 506-16-11-02-00-21 |
| | 11. Contract or Grant No. |
| 12. Sponsoring Agency Name and Address | 13. Type of Report and Period Covered |
| National Aeronautics and Space Administration<br>Washington, D.C. 20546 | Technical Memorandum |
| | 14. Sponsoring Agency Code |

15. Supplementary Notes

16. Abstract

New, direct evidence is reported for the simultaneous occurrence of Ostwald ripening and short-distance cluster mobility during annealing of discontinuous metal films on clean amorphous substrates. The anneling characteristi s of very thin particulate deposits of silver on amorphized clean surfaces of single crystalline thin graphite substrates have been studied by *in-situ* transmission electron microscopy (TEM) under controlled environmental conditions (residual gas pressure of $10^{-9}$ torr) in the temperature range from 25 to 450°C. It was possible to monitor all stages of the experiments (i.e., sputter cleaning of the substrate surface, metal deposition, and annealing) by TEM observation of the same specimen area. Various techniques (e.g., pseudostereographic presentation of micrographs in different annealing stages, the observation of the annealing behavior at cast shadow edges, and measurements with an electronic image analyzing system) were employed to aid the visual perception and the analysis of changes in deposit structure recorded during annealing. Slow Ostwald ripening was found to occur in the entire temperature range, but the overriding surface transport mechanism was short-distance cluster mobility. This was concluded from *in-situ* observations of individual particles during annealing and from measurements of cluster size distributions, cluster number densities, area coverages, and mean cluster diameters.

| 17. Key Words (Suggested by Author(s)) | 18. Distribution Statement |
|---|---|
| Cluster mobility, island films, in-situ electron microscopy, surface mass transport | Unlimited<br><br>STAR Category<br>72, 76, 77 |

| 19. Security Classif. (of this report) | 20. Security Classif. (of this page) | 21. No. of Pages | 22. Price* |
|---|---|---|---|
| Unclassified | Unclassified | 28 | $3.75 |

*For sale by the National Technical Information Service, Springfield, Virginia 22151

# DIRECT OBSERVATION OF SMALL CLUSTER MOBILITY AND RIPENING

Klaus Heinemann and Helmut Poppa

Ames Research Center, NASA, Moffett Field, California 94035 (U.S.A.)

## SUMMARY

New, direct evidence is reported for the simultaneous occurrence of Ostwald ripening and short-distance cluster mobility during annealing of discontinuous metal films on clean amorphous substrates. The annealing characteristics of very thin particulate deposits of silver on amorphized clean surfaces of single crystalline thin graphite substrates have been studied by *in-situ* transmission electron microscopy (TEM) under controlled environmental conditions (residual gas pressure of $10^{-9}$ torr) in the temperature range from 25 to 450°C. It was possible to monitor all stages of the experiments (i.e., sputter cleaning of the substrate surface, metal deposition, and annealing) by TEM observation of the same specimen area. Various techniques (e.g., pseudostereographic presentation of micrographs in different annealing stages, the observation of the annealing behavior at cast shadow edges, and measurements with an electronic image analyzing system) were employed to aid the visual perception and the analysis of changes in deposit structure recorded during annealing. Slow Ostwald ripening was found to occur in the entire temperature range, but the overriding surface transport mechanism was short-distance cluster mobility. This was concluded from *in-situ* observations of individual particles

/

during annealing and from measurements of cluster size distributions, cluster number densities, area coverages, and mean cluster diameters.

## INTRODUCTION

Within the framework of studies aiming at a better understanding of the interaction mechanism of atoms with solid surfaces, the question of mobility of atom clusters on single crystalline or amorphous substrates has been addressed by several investigators[1-6]. The results reported indicate that considerable discrepancies exist between the experimental findings and in the interpretations of substrate/deposit interactions at the substrate-adatom cluster interface. In early studies, G. A. Bassett[1] observed the rotation and possible translation of large clusters of silver (100 to 1000 Å) on molybdenite and graphite. Sears and Hudson[2] argued that spontaneous thermal mobility of large clusters is not a feasible explanation for Bassett's experiments. They suggest that due to the poor vacuum conditions, a film of contaminants had formed between the silver clusters and the substrate, and that this film had affected, in an uncontrolled manner, the adatom-substrate bonding conditions. D. W. Bassett[3] later showed theoretically that the mobility of atom clusters should be considerably less than the mobility of single adatoms (e.g., the mobility of a nine-atom cluster should be less than 1% of the mobility of a single adatom). As reasons for the observed high mobility of some clusters, he suggested (a) a weak inter-atom bonding in the clusters, or (b) a

weakening of the adatom-substrate bonding due to the inter-adatom bond formation.

Métois *et al.*[4] conducted extensive studies of the mobility of 20 to 40 Å gold and aluminum clusters on KCl substrates. They analyzed the particle density distribution $C(x,t)$ as a function of the distance $x$ from a cast shadow edge, and of annealing time $t$ for different annealing temperatures. They found a significant decrease of the slope of $C(x,t)$ with increase in annealing time and temperature, which would indicate that some clusters had migrated more than 1000 Å. Robertson[5] estimated that in the case of a migration mechanism of small crystallites, one would expect a decrease in the number of clusters and an increase in the average size. The fact that Métois *et al.*[4] did not observe such changes would indicate that either coalescence is inhibited at the lower temperatures (<150°C), or the clusters do not in fact move as entities. Robertson rationalized the inhibition of coalescence as a consequence of electrostatic or elastic interaction between the crystallites. The latter mechanism involves overgrowth-induced substrate lattice strains and is, therefore, strongly dependent on the deposit/substrate system chosen for the experiments.

Schwabe and Hayek[6] were not able to reproduce the results of Métois *et al.*[4]. Both groups of researchers used indirect methods to detect density profile changes along shadow edges, characterized

by fixing particular annealing stages with a replicating Ta/W or C film.

Clearly, the most direct and promising approach to detect and measure particle mobilities is by performing the entire surface cleaning, deposition, and annealing experiment under constant electron microscope control if effects of the imaging electron beam can be shown to not appreciably affect the processes to be studied. Honjo *et al.*[7] recently reported results of *in-situ* mobility studies of palladium and gold clusters on (001) and (111) MgO cleavage faces. They observed cluster mobilities of less than 20 Å within a period of 20 min, which is more than one order of magnitude less than the value reported by Métois *et al.*[4]. Possible principal limitations of Honjo's approach can be seen in the vacuum conditions ($10^{-8}$ torr range), the lack of surface cleaning facilities other than very high electron beam intensity induced surface cleavage, and inaccuracy in the determination of the deposition parameters.

The intent of a series of systematic investigations, of which the present studies constitute an introductory part, is to perform annealing experiments *in situ* under highly controlled conditions, with improved EM resolution and specimen cleanliness in an analyzed residual gas environment, and with reduced electron beam dosages. Amorphized single crystalline graphite films were used as substrates onto which silver clusters of 14 Å mean diameter were deposited.

Individual clusters of less than 10 Å in diameter were included in the evaluation which was, in part, performed with an electronic particle size analyzer.

The use of single crystalline support films is essential if clusters of less than 10 Å in diameter are to be imaged and if their behavior on the substrate surface is to be studied. This is due to the phase contrast background structures, which are inherent to images of amorphous support films and which stem from the nonlinearity in the phase contrast transfer characteristic in the normal bright field mode of EM operation[8,9]. Mihama *et al.*[10] adopted the use of a noise-free support film and demonstrated clearly that gold particles of less than 10 Å in diameter, grown on NaCl and extracted by a single crystalline BeO support film, can be imaged. The studies reported here were performed on single crystalline graphite substrates, which were exposed to a short, intensive ion bombardment cleaning treatment. This sputter process introduced bombardment damage in the top layers of the specimen, heavy enough to virtually eliminate the ordered state of the surface, but still insignificant in terms of its effect on background image noise. A prolonged sputter treatment results, however, in the amorphization of a large fraction of the entire film, which is then also clearly visible in the diffraction pattern and causes intolerable background image noise.

EXPERIMENTAL

Single crystalline graphite substrate films of several hundred Å thickness were prepared by a gelatine cleavage method first reported by Palatnik[11] and refined by Lee[12]. The films were mounted in a specimen heating stage inside the controlled vacuum of a bakeable, stainless steel chamber[13], which replaced the regular specimen chamber of a Siemens Elmiskop 101 transmission electron microscope (TEM)[14]. The specimen surface was cleaned and amorphized *in situ* by a short argon ion bombardment treatment[15] under visual electron microscope control. During sputter cleaning, the total residual background pressure, except for argon, was below $2\times10^{-8}$ torr. After completion of the sputter treatment, the total chamber pressure recovered quickly to the $10^{-9}$ torr range. A pressure of $5\times10^{-9}$ torr was then maintained throughout the entire annealing experiment.

Immediately following the ion bombardment, about 1 Å of silver was deposited at a rate of approximately 1 Å/min from an electron beam evaporator inside the UHV specimen chamber. The silver deposition was monitored by a quartz crystal microbalance. The deposition process was observed on the television monitor of a TEM image intensification system[16]. The sputter treatment and deposition were performed at an identical substrate temperature, which was varied for different experiments between room temperature and 120°C. Immediately after the completion of the silver

deposition, the values for particle number density, mean particle diameter, and mean nearest neighbor distance were $7\times10^{12}$ $cm^{-2}$, 14 Å, and 35 Å, respectively. A typical example is shown in Fig. 1(c).

The films were annealed for several hours at stepwise increasing temperatures, starting with the deposition temperature and ending at 450°C. The annealing process was usually terminated when the particle number density had decreased to about one-quarter of its original value.

After an annealing experiment was completed, the silver deposit could be removed by sputter etching, leaving a freshly cleaned, amorphous carbon surface for new experiments. This process could be repeated once or twice and then the graphite substrate film had been amorphized by ion bombardment to such a degree that intolerably strong phase contrast background structures resulted from the amorphous carbon substrate. An example of the experimental sequence of events is given in Fig. 1, where (a) indicates a final annealing stage and (b) almost complete removal of the silver particles after only 2 min of sputtering. After 1 min more of ion etching, all silver particles had disappeared except for one large cluster marked with a K. Fig. 1 (c) indicates renewed silver deposition; (d) and (e) indicate further annealing treatments up to 380°C and 450°C, respectively. The completely random arrangement of the new silver clusters,

independent of the locations of the clusters in the preceding deposition (Fig. 1(a)), is apparent. Finally, Figs. 1(f), (g), and (h) show the same specimen area after renewed sputtering for 1 min, 2 min, and 3 min, respectively. At that stage, the specimen was no longer usable for a third deposition, as the phase contrast background structures in Fig. 1(h) indicate.

Precautionary measures were taken to reduce the influence of the imaging electron beam upon the results by using an image intensification system[16] and by carefully avoiding unnecessary exposure of the specimen to the electron beam. Preliminary comparative studies after varying doses of beam exposure showed no differences in annealing behavior, which indicates that under the prevailing experimental conditions, the effect of radiation damage on the cluster mobility is probably negligible.

The experimental problem of relocating precisely the selected sample specimen areas after annealing treatments for purposes of recording the micrographs was alleviated by large and easily recognizable marker particles, which were formed in the graphite film as a result of an intensive outgassing treatment (several hours at temperatures above 450°C) prior to the first deposition. The size of these marker particles varied between 50 and 100 Å, and it was established unambiguously by stereomicroscopy and ion etching experiments that they are located inside the graphite film and not on the surface so that the annealing characteristics of

silver clusters were not influenced by these marker particles. In some annealing experiments, the number of marker particles increased during the last, high temperature stage of annealing (see, for example, in Fig. 1(d) the particles indicated with an M). In no case, however, could they be mistaken for silver clusters since the sputter etching treatment at the end of an annealing experiment clearly removed all silver clusters and left all marker particles unaffected (see Figs. 1(b) and (f) - (g)).

The electron micrographs taken at various stages of the annealing process were evaluated by statistical measurements (i.e., cluster number density and surface coverage) and by a detailed comparative analysis of location, size, and relative mobility of individual particles. An electronic image analysis system (Zeiss Videomat) was employed for the statistical analysis. Simple stereographic viewing of the same specimen area of micrographs taken at two different annealing stages proved to be an excellent means to detect changes of individual silver clusters during annealing. The other, ususally more complicated method used to detect such detailed changes was by superposition of differently colored transparencies of micrographs of different annealing stages.

RESULTS

General

A typical annealing series is shown in Fig. 2. The micrograph (a) was taken after 5 min annealing at 120°C, which also was the silver deposition temperature. Figures 2(b) and 2(c) were recorded after additional annealing at the same temperature for 28 and 109 min, respectively. The annealing at 120°C was continued for a total of 24 hr, at which time the specimen temperature was increased to 250°C. Figs. 2(d) and (e) were taken after 3 hr and 24 hr of annealing at 250°C, respectively. Easily detectable changes were only observed in the micrographs after the annealing temperature was furhter increased. Fig. 2(f) was taken after an additional 20 hr annealing at 380°C. In Fig. 3, the annealing behavior is studied at a shadow edge cast by a large impurity particle during the silver evaporation. The annealing parameters (time/temperature) were 25 min/120° for Fig. 3(a), 2 hr/120° for (b), 24 hr/120° plus 3 hr/250° for (c), additional 21 hr/250° for (d), additional 154 min/380° for (e), and additional 160 min/450° for Fig. 3(f). It is apparent that no particle movement over large distances (<100 Å) has occurred in all of these experiments, because the shadow edge in Fig. 3(f) is still well defined even after high temperature annealing. The obvious reduction in cluster number density in the later annealing stages can, therefore, only be explained by an Ostwald ripening process

and/or by a mechanism involving short-distance cluster movement that leads to coalescence. The two previously mentioned approaches of statistical and individual particle analysis were pursued for further evaluations and for a possible distinction between these two processes.

Statistical analysis

Specimen areas of about 0.02 $\mu m^2$ in size were analyzed statistically. The size distribution curves of Fig. 4(a) were extracted from histograms with 2 Å size class increments, taken from micrographs of a total of nine different annealing stages, six of which (curves a, b, c, d, e, and f) are shown in Fig. 3. The results justify a distinction between low temperature (up to 250°C) and high temperature annealing. The main change that occurred in the low temperature range was found at the very beginning of the annealing experiment (during the first hour of annealing at 120°C, Fig. 4(a), curves a and b). The entire distribution curve is shifted by almost two Å toward larger sizes, the mean particle $d_m$ increasing from 14 to 16 Å (Fig. 4(b)). This trend continued, although at a significantly lower rate of change, throughout the entire low-temperature annealing experiment. The increase of annealing temperature from 250°C to 380°C caused a significant broadening of the distribution curve, the appearance of a second (large particle) peak, and a significant increase in the half-width of the distribution curve $d_s$ which

had remained constant (10 Å) during annealing up to 250°C. The area coverage $\Delta a/a$ remained constant during low-temperature annealing while the particle number density $n$ decreased slightly (30%) during the same treatment. However, both $\Delta a/a$ and $n$ decreased simultaneously for annealing at 380 and 450°C. At the end of the annealing treatment (Fig. 3(f)), the area coverage and cluster number density have decreased to 70% and 26% of the starting values, respectively. In accordance with the principal limitations of the statistical analysis with an image analyzer, the following error limits of these results have to be considered: ±2 Å for the absolute value of the mean particle diameter, ±0.5 Å for the relative differences between the mean particle diameters of the different curves, and ±0.5 Å for the distribution half-width. The measurements for curve $d_1$ in Fig. 4(a) indicate the existence of two maxima, but there is some uncertainty. The accuracy of the particle number density measurements is within ±3%. An error of ±10% has to be applied to the area coverage measurements.

Analysis of changes of individual clusters

Upon close examination of micrographs 2 and 3 with the pseudostereoscopic or colored transparencies methods, a large number of individual events were discovered in which particles disappeared and neighboring clusters increased in volume. This would seem to indicate an Ostwald ripening mechanism and can be

seen particularly well, for example, between Figs. 2(d) and (e). The increase in area was, however, often so pronounced and much more than would be expected from a simple ripening process (see, for example, the open arrow in Figs. 2(c) and (d)) that the conclusion seems justified that in these cases the formerly separated clusters have moved toward each other without sintering into one single, larger crystallite. Model mechanisms that would explain these observations are schematically illustrated in Fig. 5. If cluster mobility is the operating mechanism for the second type of observations, it can be expected that in some cases *both* particles move, and that the new particle is situated between the former cluster positions. This was, in fact, observed repeatedly even for low-annealing temperatures (see, for example, the center solid arrow in Figs. 2(a) and (b)). The mobility of small clusters of atoms, although over only very small distances (usually <20 Å) as one possible mechanism in the coalescence process at relatively low temperatures is, therefore, directly confirmed by these observations.

To examine more closely the existence of Ostwald ripening as another viable surface mass transport mechanism, an annealing experiment was conducted during which a large number of micrographs were recorded in rapid sequence from the TV monitor of the image intensification system. A number of characteristic stages of this experiment are shown in Fig. 6. The solid arrows indicate

three different locations, at which the *gradual* decrease in size and the final disappearance of a cluster of approximately 15 Å in diameter can be observed. The process of ripening was, in all three cases, observed over periods of several minutes.

## DISCUSSION

### Ripening

It has been suggested[17] that the ripening process is slow and will, therefore, be of significance only during annealing and not during the deposition of a thin discontinuous film. The present observations, that the Ostwald ripening processes take place over periods of more than $10^3$ sec, support the concept of a slow speed process. According to Chakraverty[18], the size distribution in ripened discontinuous films is a distinct asymmetric $\delta$-function, which is furthermore characterized by complete absence of clusters beyond twice the mean diameter in size. Both postulations are clearly not fulfilled in the present studies. The size distributions (Fig. 4(a)) have, within the limits of accuracy, Gaussian shape and show definitely the existence of large particles, the number of which increases with increasing annealing time and temperature. It can, therefore, be concluded that Ostwald ripening is not the only mechanism by which the observed decrease in cluster number density with annealing can be explained, although many individual events that support such a ripening mechanism have been found during our experiments.

Cluster mobility

The combined results of t .esent observations lead to the conclusion that cluster movement plays a significant role in the low- and high-temperature annealing behavior of silver island deposits on amorphized graphite substrate films. The specific results that support a cluster mobility model can be summarized as follows:

*(a) The development of large particle tails in the size distribution histograms (Fig. 4(a)).* This contradicts, for the reasons given in the preceding paragraph, an Ostwald ripening process as the only coalescence mechanism.

*(b) The behavior of the area coverage function (Fig. 4(b), $\Delta a/a$).* The invariance of this function in the low-temperature annealing range, when compared to the noticeable decrease of the cluster number density function (Fig. 4(b), n) in the same temperature range, indicates that clusters have moved together but not yet sintered. (The surface area occupied by a sintered coalesced particle would be less than the area originally occupied by the coalescing clusters, whereas coalescence without sintering would not affect the surface coverage.) It can, therefore, be concluded that the first stage of coalescence by cluster mobility, which is characterized by movement of the clusters toward each other until they meet, leads to a metastable condition. Sintering does not have to occur instantaneously. The fact that, during

high-temperature annealing, the area coverage d es decrease might be indicative of a thermally aided increase of the sintering rate of coalesced clusters.

*(c) The direct, visual observations of cluster movement (Fig. 7, No. 2,4,6,9).* Van der Merwe's suggestion[19] that repulsive elastic forces could serve as driving force for a surface diffusion process by which atoms are transported from the nearer to the farther sides of two small interacting islands, does not apply to the present observations. The repulsive forces introduced by Van der Merwe are due to an overlap of strain fields induced by island pairs in the substrate, and do not cause an overall movement of the islands toward each other.

*(d) The observation of small overall displacements (of a few* $\mathring{A}$ *in distance) of many small clusters within the time period between two photographic exposures.* This provides additional proof of cluster mobility. The atom-by-atom surface diffusion transport mechanism proposed by Van der Merwe[19] cannot be eliminated in this case, however.

*(e) The decrease of the cluster number density* $n$ *(Fig. 4(b)), and the corresponding slight increase of the average cluster size* $d_m$ *(Fig. 4(b)) in the low-temperature annealing range.* This agrees with Robertson's model[5] that such a behavior should be expected if, in fact, the clusters move as entities.

## CONCLUDING REMARKS

More detailed studies are clearly needed to clarify some of the still unanswered questions about the mechanisms of material transport on solid surfaces. In particular, the quantitative dependence of Ostwald ripening and cluster movement processes on annealing temperature and time remains to be explored, and the discrepancies between the large cluster mobilities observed by Métois *et al.*[4] and the minute mobilities observed in the present studies, and by Honjo[7] and Schwabe and Hayek[6] need to be resolved. These studies must include both highly accurate, statistical, nearest-neighbor measurements and evaluations of individual particle changes at short time intervals during *in-situ* annealing experiments in a clean environment.

REFERENCES


1. G. A. BASSETT, Proc. Europ. Reg. Conf. Electr. Micr. Delft (1960) Vol. 1, p. 270.
2. G. W. SEARS and J. B. HUDSON, *J. Chem. Phys.*, *39* (1963) 2380.
3. D. W. BASSETT, *Surf. Sci.*, *23* (1970) 240.
4. A. MASSON, J. J. MÉTOIS, and R. KERN, *Surf. Sci.*, *27* (1971) 463 and 483; J. J. MÉTOIS, M. GAUCH, A. MASSON, and R. KERN, *Surf. Sci.*, *30* (1972) 43; J. J. MÉTOIS, *Surf. Sci.*, *36* (1973) 269.
5. D. ROBERTSON, *J. Appl. Phys.*, *44* (1973) 3924.
6. U. SCHWABE and K. HAYEK, *Thin Solid Films*, *12* (1972) 403.
7. G. HONJO, K. TAKAYANAGI, K. KOBAYASHI, and K. YAGI, Proceed. 4th Intl. Conf. Cryst. Growth (1974) 98, and Proceed. 6th Intl. Vac. Congr. 1974, Jap. J. Appl. Phys. Suppl. 2, Pt. 1 (1974) 537.
8. O. SCHERZER, *J. Appl. Phys.*, *20* (1949) 20; *F. THON., Z. Naturforsch., 21a (1966) 476.*
9. H. POPPA, Epitaxial Growth, Part A, Academic Press, Inc. San Francisco 1975, p. 215.

   K. MEINMANN, *Optik*, *33* (1971) 113.
10. K. MIHAMA, S. SKIMA, and R. UYEDA, Proceed. 4th Int'l Conf. Cryst. Growth (1974) 100.
11. L. S. PALATNIK, V. M. KOSEVICH, L. P. ZOZULYA, L. F. ZOZULUYA, and V. K. SOROKIN, *Sov. Phys.*, *11* (1970) 2086.

12. E. LEE, Ph.D. thesis, Stanford Univeristy, 1974.

13. R. D. MOORHEAD and H. POPPA, Proc. 27 EMSA Meeting (1969) 116.

14. K. HEINEMANN, D. B. RAO, and D. L. DOUGLASS, *Oxid. of Met.*, 9 (1975) 379.

15. K. HEINEMANN and H. POPPA, *J. Vac. Sci. Technol.*, 10 (1973) 22.

16. K. HEINEMANN and H. POPPA, Proc. 30th EMSA Meeting (1972) 610 and 612.

17. G. ZINSMEISTER, Proc. 6th Int'l Vacuum Congr. 1974, Japan J. Appl. Phys. Suppl. 2, Pt. 1 (1974) 545.

18. B. K. CHAKRAVERTY, *J. Phys. Chem. Solids*, 28 (1967) 2401.

19. J. H. VAN DER MERWE, 4th Int'l Conf. Cryst. Growth (1974) 163.

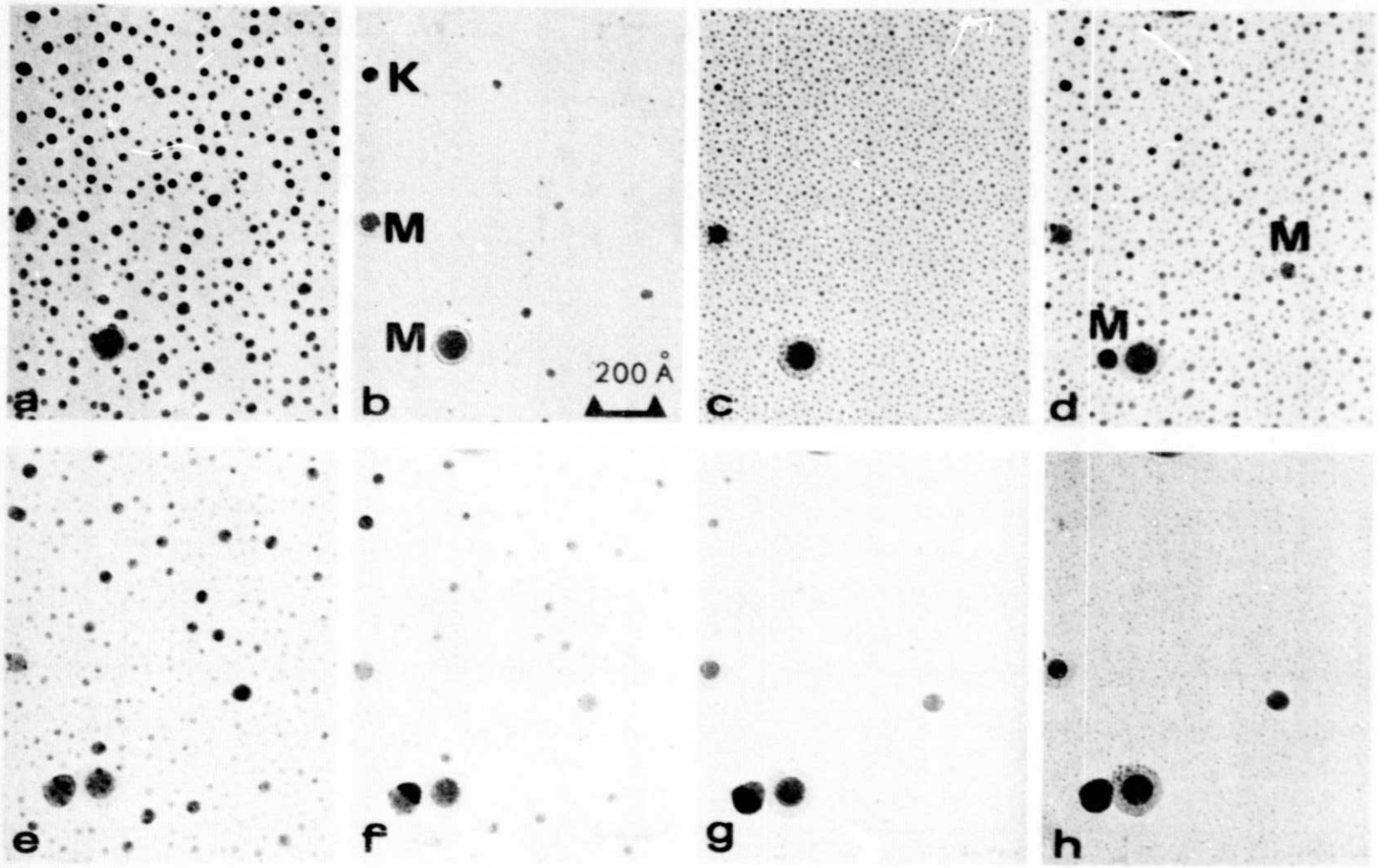


Fig. 1. Selected area of a thin graphite film with large marker inclusions M subjected to various successive etching, deposition, and annealing treatments; for details, see text.

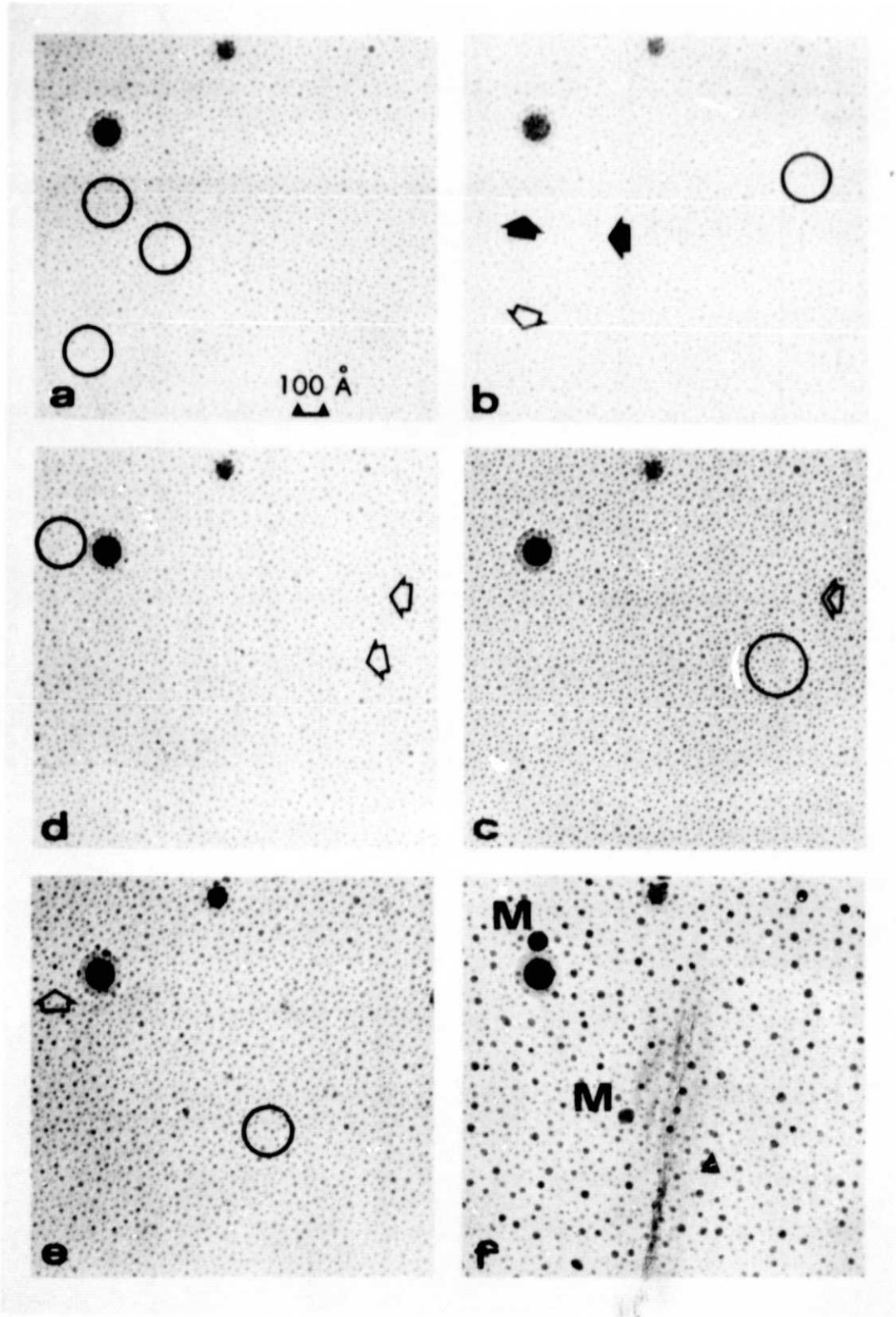


Fig. 2. Typical annealing series of silver clusters evaporated at 120°C onto an amorphized graphite substrate. The micrographs are arranged for viewing of particle changes with a stereo viewer. The arrows point to areas where specific changes have occurred with respect to the corresponding details within the encircled areas in the preceding micrographs.

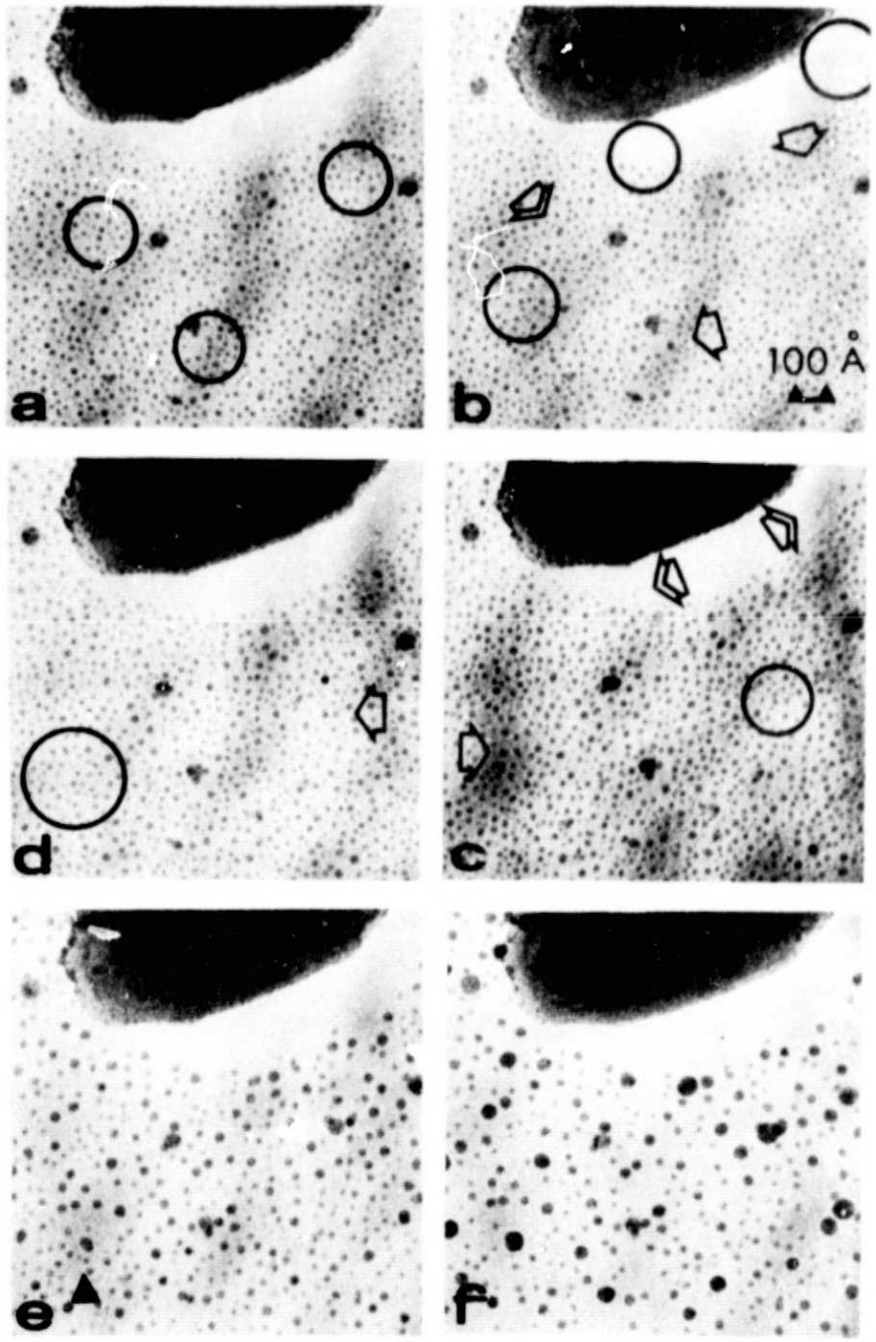


Fig. 3. Demonstration of the annealing characteristics of silver clusters at a cast shadow edge (see text for details), arranged for pseudostereo viewing.

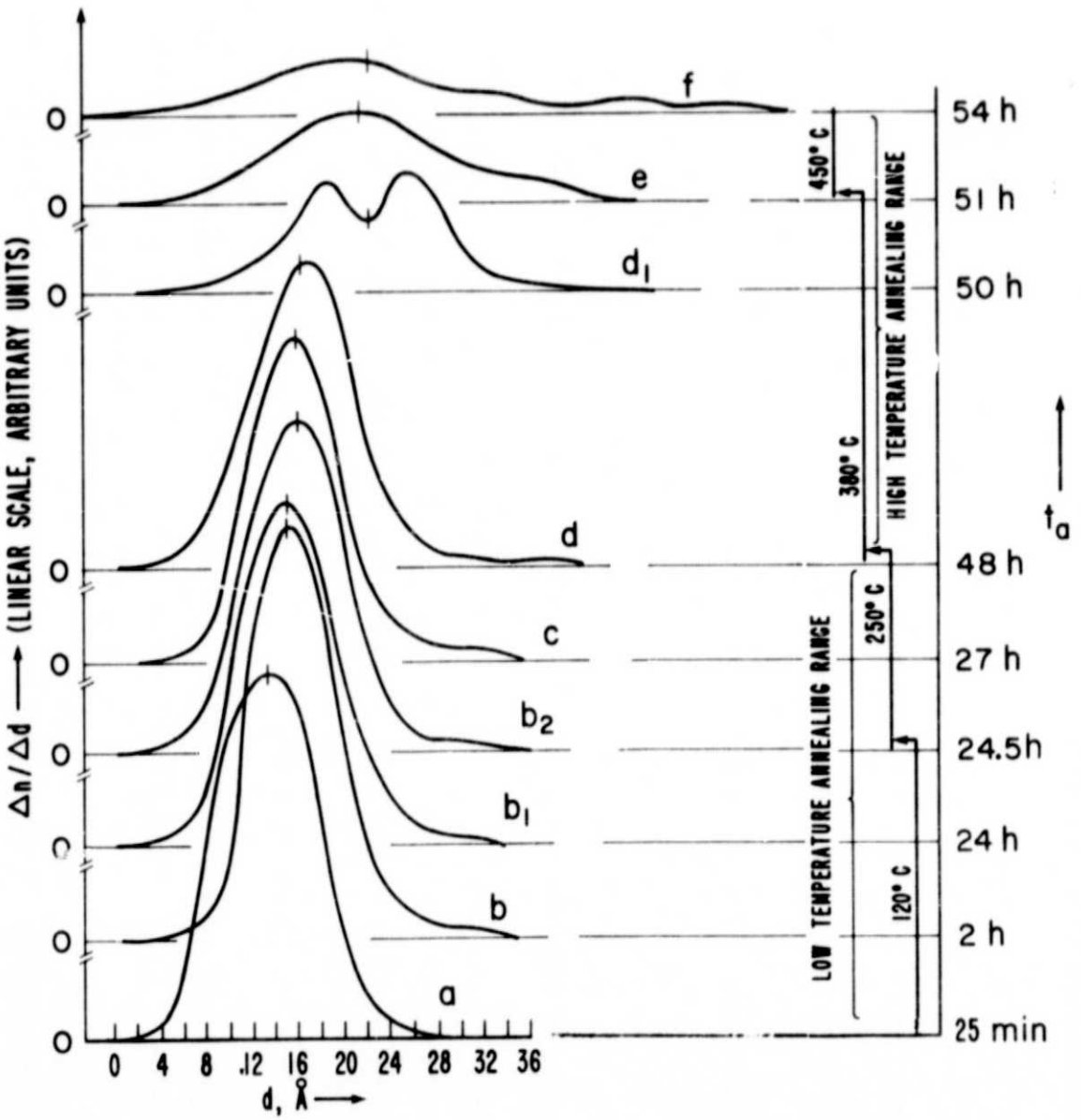


(a) size distributions $\Delta n/\Delta d$.

Fig. 4. Results of the statistical analysis of nine micrographs taken successively during an annealing experiment.

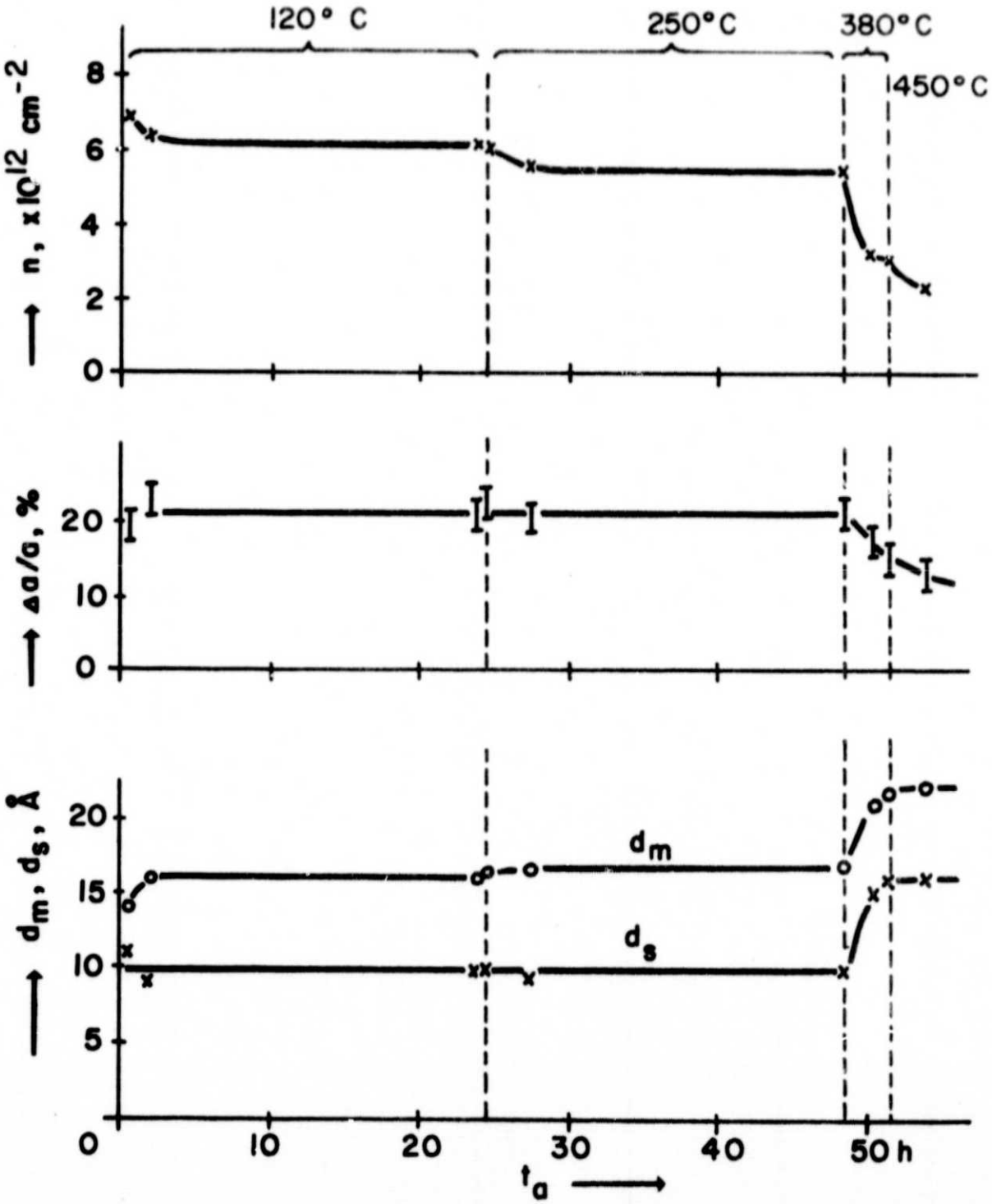


(b), half-width of size distribution $d_s$, mean cluster diameter $d_m$, area coverage $\Delta a/a$, and cluster number density n.

Fig. 4. Concluded.

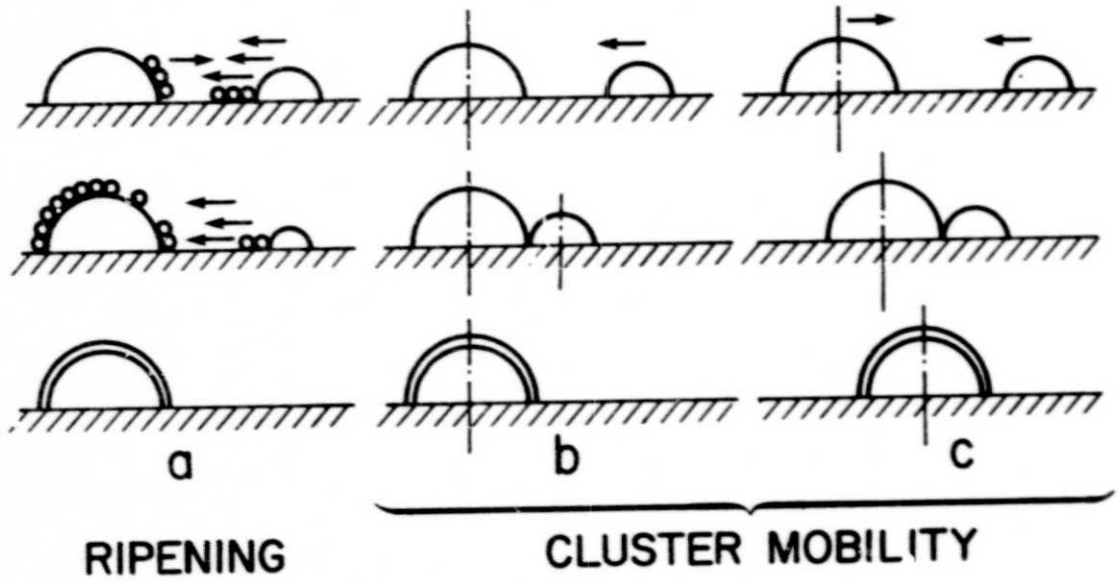


Fig. 5. Coalescence mechanism (a) by Ostwald ripening, (b) by cluster mobility (one cluster moves), and (c) cluster mobility (both clusters move). For (b) and (c), the middle and lower rows indicate the cluster movement phase and the sintering phase, respectively.

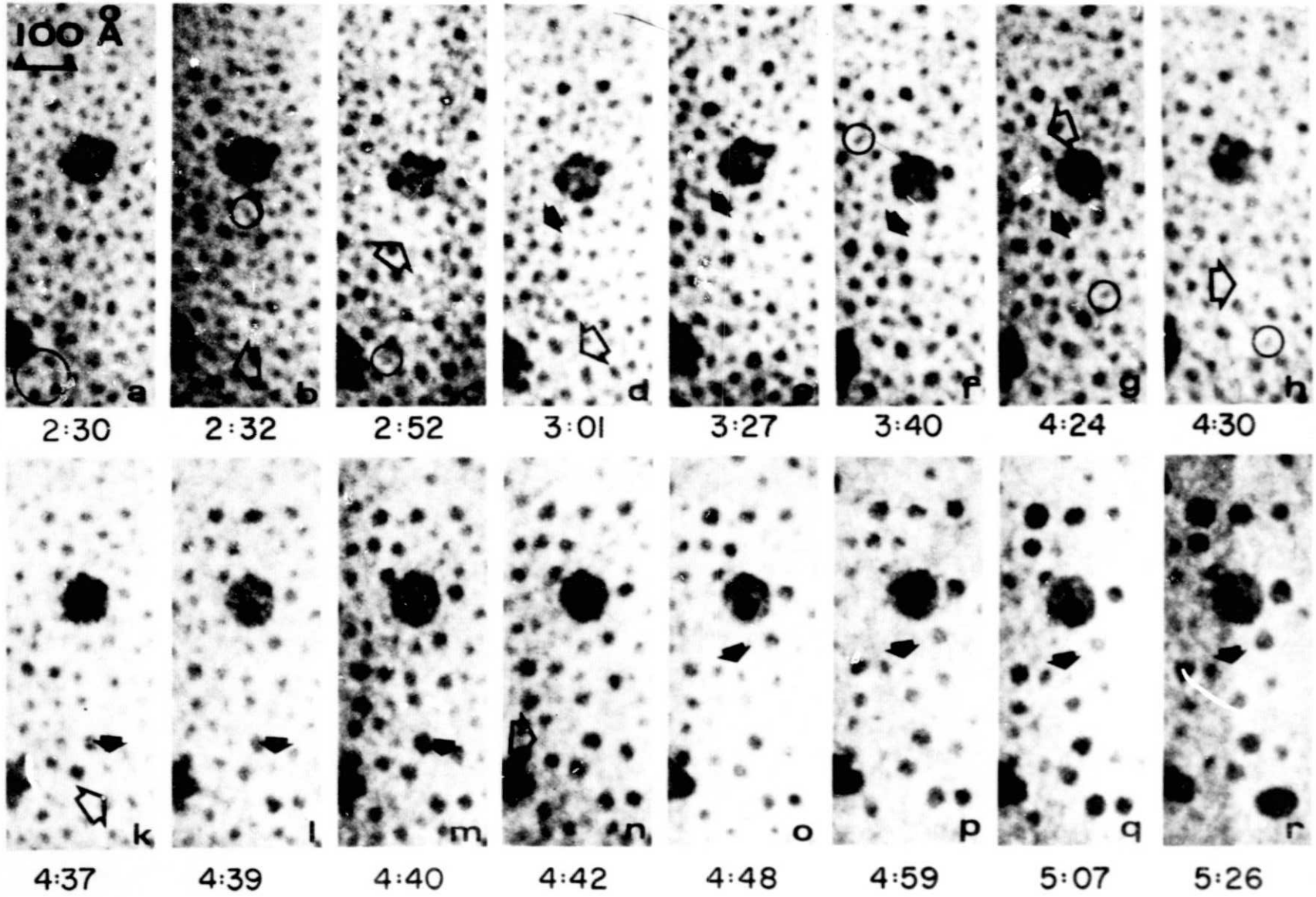


Fig. 6. High magnification annealing sequence; slow Ostwald ripening is specifically indicated by solid arrows. The temperatures during annealing were: 25°C until 2:35; 120° from 2:36 until 3:02; 220° from 3:03 until 3:27; 320° from 3:28 until 3:35; 380° from 3:36 to 4:27; and 450° starting at 4:28.

| No. | Before | After | Description of process | Typical examples | Mechanism | Special remarks |
|---|---|---|---|---|---|---|
| 1 |  |  | one cluster disappears, another grows spherically | Fig. 2 e,f, all over<br>Fig. 3 c,d, open arrow<br>Fig. 3 e,f, all over<br>Fig. 6, open arrows | ripening and/or coalescence by cluster movement followed by sintering | often difficult to distinguish; sometimes, first No.2 was observed, followed by sintering in next exposure (Fig. 1 b,c,d, arrows) |
| 2 | 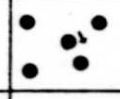 | 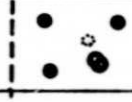 | one cluster disappears, another grows, with evidence of both remaining | Fig. 2 c,d, open arrow<br>Fig. 3 a,b, open arrows<br>Fig. 3 b,c, open arrow | coalescence by cluster movement without sintering | |
| 3 | 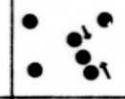 | 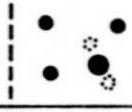 | two or more clusters disappear, a center cluster grows | Fig. 2 a,b, open arrow<br>Fig. 2 e,f, all over<br>Fig. 3 d-f, all over | same as No. 1, involving several particles | observed mostly at high annealing temperatures |
| 4 | 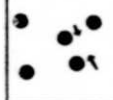 | 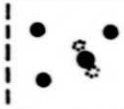 | two clusters move to a new place in between previous locations | Fig. 2 a,b, solid arrows<br>Fig. 6 a,b, open arrow | coalescence by simultaneous movement of two clusters | observed frequently |
| 5 |  | 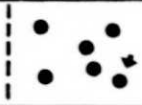 | a new particle appears without evidence of previous location | Fig. 3 b,c, double arrows | cluster movement (<50 Å) | rarely observed |
| 6 |  | 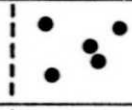 | one cluster moves closer to another cluster and stops there | Fig. 3 a,b, double arrow<br>Fig. 3 b,c, open arrow | cluster movement (<30 Å) | observed less frequently |
| 7 |  | 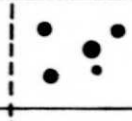 | a cluster disappears slowly, observed over several exposures | Fig. 6 d-g, solid arrows<br>Fig. 6 k-m, solid arrows<br>Fig. 6 o-r, solid arrows | slow Ostwald ripening | observed for low and high temperatures |
| 8 | 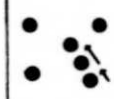 | 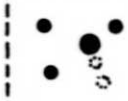 | two clusters coalesce and then move on to coalesce with a third cluster | Fig. 2 d,e, open arrow | coalescence in two successive stages | rarely observed |
| 9 |  | 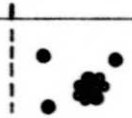 | the space between two clusters fills by movement, yet no sintering takes place. | Fig. 2 e,f, solid triangle.<br>Fig. 3 d,e, solid triangle. | coalescence by movement of several clusters (without sintering) | observed seldom, but even at higher annealing temperatures. |

Fig. 7. Summary of observations of individual cluster changes during annealing.